Temporal Uplift Modeling for Online Marketing

Xin Zhang*†
Wuhan University
Wuhan, China
zhangxin@whu.edu.cn

Kai Wang*
NetEase Fuxi AI Lab
Hangzhou, China
wangkai02@corp.netease.com

Zengmao Wang‡†
Wuhan University
Wuhan, China
wangzengmao@whu.edu.cn

Bo Du‡†
Wuhan University
Wuhan, China
dubo@whu.edu.cn

Shiwei Zhao
NetEase Fuxi AI Lab
Hangzhou, China
zhaoshiwei@corp.netease.com

Runze Wu‡
NetEase Fuxi AI Lab
Hangzhou, China
wurunze1@corp.netease.com

Xudong Shen
NetEase Fuxi AI Lab
Hangzhou, China
hzshenxudong@corp.netease.com

Tangjie Lv
NetEase Fuxi AI Lab
Hangzhou, China
hzlvtangjie@corp.netease.com

Changjie Fan
NetEase Fuxi AI Lab
Hangzhou, China
fanchangjie@corp.netease.com

ABSTRACT

In recent years, uplift modeling, also known as individual treatment effect (ITE) estimation, has seen wide applications in online marketing, such as delivering one-time issuance of coupons or discounts to motivate users' purchases. However, complex yet more realistic scenarios involving multiple interventions over time on users are still rarely explored. The challenges include handling the bias from time-varying confounders, determining optimal treatment timing, and selecting among numerous treatments. In this paper, to tackle the aforementioned challenges, we present a temporal point process-based uplift model (TPPUM) that utilizes users' temporal event sequences to estimate treatment effects via counterfactual analysis and temporal point processes. In this model, marketing actions are considered as treatments, user purchases as outcome events, and how treatments alter the future conditional intensity function of generating outcome events as the uplift. Empirical evaluations demonstrate that our method outperforms existing baselines on both real-world and synthetic datasets. In the online experiment conducted in a discounted bundle recommendation scenario involving an average of 3 to 4 interventions per day and hundreds of treatment candidates, we demonstrate how our model outperforms current state-of-the-art methods in selecting the appropriate treatment and timing of treatment, resulting in a 3.6% increase in application-level revenue.

*Co-first authors
†Also with the National Engineering Research Center for Multimedia Software, Institute of Artificial Intelligence of Wuhan University, and the Hubei Key Laboratory of Multimedia and Network Communication Engineering.
‡Corresponding authors

Permission to make digital or hard copies of all or part of this work for personal or classroom use is granted without fee provided that copies are not made or distributed for profit or commercial advantage and that copies bear this notice and the full citation on the first page. Copyrights for components of this work owned by others than the author(s) must be honored. Abstracting with credit is permitted. To copy otherwise, or republish, to post on servers or to redistribute to lists, requires prior specific permission and/or a fee. Request permissions from permissions@acm.org.
KDD '24, August 25–29, 2024, Barcelona, Spain
© 2024 Copyright held by the owner/author(s). Publication rights licensed to ACM.
ACM ISBN 979-8-4007-0490-1/24/08
https://doi.org/10.1145/3637528.3671560

CCS CONCEPTS

• **Information systems** → **Personalization**; • **Applied computing** → **Online shopping**.

KEYWORDS

online marketing, uplift modeling, individual treatment effect

ACM Reference Format:
Xin Zhang, Kai Wang, Zengmao Wang, Bo Du, Shiwei Zhao, Runze Wu, Xudong Shen, Tangjie Lv, and Changjie Fan. 2024. Temporal Uplift Modeling for Online Marketing. In *Proceedings of the 30th ACM SIGKDD Conference on Knowledge Discovery and Data Mining (KDD '24), August 25–29, 2024, Barcelona, Spain.* ACM, New York, NY, USA, 10 pages. https://doi.org/10.1145/3637528.3671560

1 INTRODUCTION

In modern online marketing, uplift modeling has emerged as a pivotal technique for enhancing user engagement and platform revenue by offering targeted incentives (i.e., treatment) such as coupons [31] and discounts [15]. Traditional marketing strategies often overlook the likelihood of a customer purchasing a product without any intervention (i.e., giving treatment). This oversight has prompted a paradigm shift towards uplift-based strategies that prioritize marketing actions to induce a significant uplift in user purchases, rather than merely focusing on items with the highest probability of purchase. Consider the following scenario: during a marketing campaign, the system predicts a 90% probability of a user purchasing bottled water and a 40% probability for an energy drink. Traditional strategies would favor bottled water due to its higher purchase probability. However, without intervention, bottled water might still have an 80% purchase likelihood due to its essential nature, while the energy drink might only have a 10% likelihood. In this case, recommending the energy drink could be more strategic, as it represents a greater increase in purchase probability (30% vs. 10%), potentially leading to higher profits. Considering that these incentives carry costs and that diverse users respond differently to them — where some only purchase with coupons, while others would purchase regardless — accurately identifying the sensitive

user segments for each incentive is crucial for maximizing marketing efficacy. Unlike traditional supervised learning, this involves a typical causal inference problem, as we cannot observe both the factual outcome (what actually happened) and the counterfactual outcome (what would have happened under a different decision) for an individual simultaneously. To achieve this objective, online marketing employs estimation of individual treatment effects (ITE) or uplift to accurately capture the differential response of users to various incentives compared to no incentives. Uplift modeling has been validated across multiple scenarios [3, 6].

Existing uplift modeling methods for online marketing can be categorized into the meta-learner method [13, 20], the tree-based approach [22, 26], and neural network-based approach [23, 25]. The main idea is to predict unbiased outcomes of different treatments by establishing a connection between treated and controlled groups [11], accomplished through the implementation of various data utilization methods [20] and subpopulation segmentation [22]. While existing uplift modeling methods have demonstrated promising results in simple scenarios, such as one-time treatment, most cannot be applied in scenarios where users receive more than one treatment across a continuous timeline. A typical online marketing scenario is depicted in Figure 1(a), where users have historical temporal data on treatments and outcomes, posing three challenges:

- **Highly biased data.** Users' responses to past treatments shape future treatments, resulting in a higher bias in sequential scenarios compared to static single-intervention scenarios. For instance, based on learning from past data, the system perpetually recommends high-value discounts to high-spending users, and users develop strong expectations regarding discount values. The direct use of sequence learning methods [12, 27] will be biased by the highly biased data and will not be able to make accurate estimations of counterfactuals for different treatments.
- **Handling time-varying confounders.** In Figure 1(a), the user is given the treatment f_3 at t_3, assuming the user's covariate itself was influenced by past treatment f_2, failing to adjust for time-varying confounders (the impact of f_2 on user covariates) would lead to erroneous conclusions about the effectiveness of treatment f_2 if the user exhibits purchase behavior after f_3 rather than after f_2. Existing uplift-based methods [16, 20] solely considering treatments and outcomes dependent on static user covariate values are inadequate for estimating the effect of a sequence of treatments on user outcomes.
- **Continuous-time modeling.** In online marketing, the occurrence of multiple events within a time window, including treatments and outcomes, is common. A user's outcome event can be attributed to multiple treatments within a time window. Time gap is a critical factor in estimating the mutual influence of treatment and outcome effects, with effects generally diminishing over time. Since uplift is defined as the change in the distribution of future outcomes due to treatment, the impact of treatment on future outcomes at different time points needs to be estimated and integrated over time. Point process models [5, 7] are considered effective techniques for handling the mutual influence of events on continuous-time event sequences.

In this paper, to tackle the aforementioned challenges, we propose a novel Temporal Point Process-based Uplift Model, denoted as TPPUM. As shown in Figure 1(b), it models the individual treatment effect of a treatment given at timestamp t_5 on a user's future outcome through counterfactual reasoning on temporal point processes. Initially, we define a causal model that characterizes the uplift as the effect of the treatment on altering the intensity function of user purchases. Here, the marketing action is considered the treatment, and the user's future conditional intensity function is regarded as the outcome. To address bias stemming from time-varying confounders in the point process, we draw inspiration from CRN [4] and employ domain adversarial training to establish balancing representations of the user's past event sequence. Furthermore, we extend this approach from discrete time-step event sequences to continuous time event sequences. Given an event occurs at timestamp t, TPPUM first constructs a time-aware treatment-invariant representation for the user's historical events preceding that particular event. The resulting balancing representation, denoted as H, is then utilized to separately model the intensity function $\lambda(t|H)$ and the event's feature distribution $p(f|H)$ using temporal point processes and Multi-layer Perceptron (MLP), respectively. The parameters $\lambda(t|H)$ and $p(f|H)$ are learned by maximizing the likelihood of each event given the user's past event sequence. By directly learning the integrated intensity function, our model allows for obtaining a closed-form solution for the expectation of the outcome distribution, thereby enhancing efficiency in model inference.

We summarize the main contributions as follows:

- We first explore temporal uplift modeling for online marketing, extending uplift modeling scenarios from single-step intervention to multiple interventions across a continuous timeline. We introduce a novel causal model that quantifies the causal effect of treatments at specific timestamp t. Additionally, we develop a neural temporal process model that enables unbiased estimation of these effects.
- We deploy the model in a challenging real-world online marketing application. This scenario is significant and innovative due to its realistic setting, allowing for multiple interventions over time and requiring decision-making from hundreds of treatment options, including timing and content. The sophisticated estimation of uplift enables an optimal equilibrium between bundle GMV and shop GMV, thereby achieving a 3.7% uplift in application-level revenue.

2 RELATED WORK

2.1 Uplift Modeling For Online Marketing

The uplift modeling has evolved along three distinct research lines: 1) meta-learner method leverages existing techniques to construct

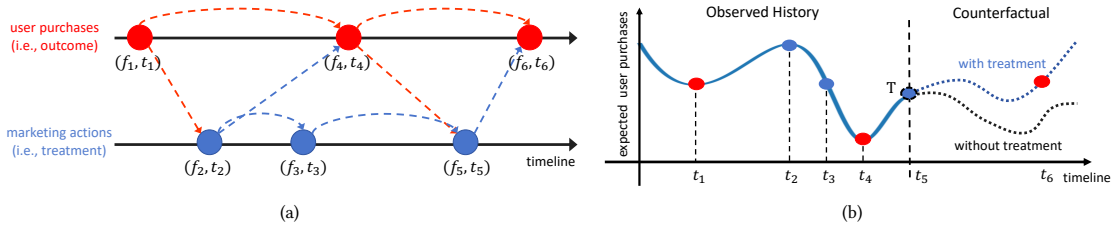

Figure 1: (a) depicts a typical scenario of online marketing. On one hand, purchasing (i.e., outcomes) trigger each other on the timeline based on their individual dynamics. On the other hand, marketing actions (i.e., treatment) impact the future purchasing within a certain time window. (b) depicts changes in the expected value of user purchases over time. At a current time t_5, the model can predict the counterfactual dynamic (the colored dashed branches) with planned treatments and the dynamic (the black dashed branches) without treatments.

potential outcome models separately for the treatment and control groups [13, 20]. 2) Tree-based methods [22, 26] explicitly divide sensitive users corresponding to each treatment using different metrics as splitting criteria, offering interpretability. 3) Neural network-based methods leverage the advantages of neural networks to capture more complex and flexible relationships between treatments and outcomes. With neural networks, models could learn more unbiased information from observed data [23, 25]. Furthermore, some studies focus on utilizing deep learning to eliminate the effect of confounders [17, 28]. Some studies pay more attention to utilizing extra information for uplift estimation. For example, DESCN [32] introduces the entire space from multi-task learning to address distribution imbalance. EFIN [16] encodes not only user and contextual features but treatment features. These methods can only be applied to single-intervention scenarios in a static setting.

2.2 Causal Inference Over Time

Beyond the realm of uplift in online marketing, a few studies pay attention to the sequence-to-sequence methods for estimating the treatment effect in a dynamic view. Here, RMSN [14] uses RNN to predict the inverse probability of treatment for training networks. CRN [4] uses adversarial learning to produce balanced representations, which are simultaneously predictive of the outcome but non-predictive of the current treatment assignment. DCRN [2] disentangles the balancing representations into treatment, outcome and confounder factor. CT [19] utilizes a Transformer into sequence encoding. These models are mainly intended for medical situations where treatment and outcome events occur concurrently. While we have adapted these algorithms to support temporal sequence in the experimental section, due to their architecture, calculating the uplift value of treatment on future outcomes remains a challenge for these algorithms.

2.3 Temporal Point Process

Temporal point processes (TPP) have gained attention as versatile tools for generating sequences of discrete events in a continuous timeline, finding applications across various domains [18, 24]. Recently, the applications of neural networks in point process modeling have attracted significant attention. RMTPP [7] introduces recurrent neural networks instead of specifically fixed assumptions to view the intensity function of a temporal point process. JUMP [33] uses point process and sequential modeling techniques to predict dwell time based on three-layered RNN. CNTPP [30] incorporates the neural point process and Gaussian mixture models to estimate the ITE of misinformation on social media.

3 PRELIMINARY

3.1 Temporal Uplift Problem Definition

Consider an observational dataset $D = (X^i, a^i, y^i, T^i)_{i=1}^N$ consisting of history events about N samples. For i-th sample (each sample is an outcome event), $X^i = [f_1^i, f_2^i, ..., f_L^i]$ and $T^i = [t_1^i, t_2^i, ..., t_L^i]$ is the sequence of history events features and corresponding timestamp. $f_l^i \in R^{d_f}$ is a vector indicates d_f features of the l-th event. L means the total number of events in sequence. $a^i \in R^{d_a}$ is a vector that indicates which treatment option (also including the option of no treatment) has been employed in i-th sample. y^i indicates the actual outcomes. Choosing what feature of outcome events as outcome y^i usually depends on the actual task. As depicted in Figure 1b, our goal is to estimate the causal effect of the previous treatment event on the outcome event over time. Consequently, followed by [30], the employed treatment option a^i is decided by the last event. Specifically, if the previous event is a treatment event, we consider that the current outcome event receives the corresponding treatment. If the previous event is an outcome event, we consider that the current event receives no treatment. For simplicity, the superscript i will be omitted in the later part.

Following the potential outcome framework [8, 21], let $y(\hat{a})$ and $y(0)$ be the potential outcomes for each possible option of treatment $\hat{a}$ and for no treatment respectively. Then the objective of this paper is to estimate the uplift of the treatment $\hat{a}$ for each outcome event at the target timestamp which is defined as $\tau(\hat{a}, t^*) = y(\hat{a}, t^*) - y(0, t^*)$. However, we only have access to a single observed outcome, which poses a challenge for uplift modeling as it differs from traditional supervised learning. Thus, for each user, the goal of uplift modeling is to estimate the expected ITE $\tau(\hat{a}, t^*)$ of each treatment $\hat{a}$ given history events X and timestamp T. It can be formulated as:

$$\tau(\hat{a}, t^*) = E(y|a = \hat{a}, t = t^*, X, T) - E(y(0)|a = 0, t = t^*, X, T) \quad (1)$$

After obtaining all the ITE $\tau(\hat{a}, t^*)$ for each of the treatment options $\hat{a}$ and the candidate target timestamp t^*, we can rank these estimated ITEs and select the optimal treatment timestamp to assign an effective treatment.

3.2 Marked Temporal Point Process

The marked temporal point process is a highly effective framework for capturing the underlying mechanisms that govern the observed patterns of random events over time [7]. By considering the temporal dependencies among events, we can develop models that explicitly account for the influence of past events on the timing of future events. More formally, a marked temporal point process represents a random process characterized by a sequence of discrete events, each associated with a specific timing, denoted as t, and a marker, denoted as f. In this paper, we assign the marker of an event (both treatment and outcome) as its associated features. In this paper, the marker f can be regarded same as feature f in section 3.1.

By considering the historical sequence of events, we can explicitly characterize the marked temporal point process using the conditional intensity function $\lambda(f, t|H)$ that the next event will happen at time t with marker f where $H = (X, T)$ is the historical sequence of events and corresponding timestamp before t. The intensity function $\lambda(f, t|H)$ means the instantaneous probability of the event occurring at time t with marker f [5]. Based on the intensity function, we can derive the probability density function for the j-th event, which occurs at time t_j with marker f_j:

$$p(f_j, t_j|H_j) = \lambda(f_j, t_j|H_j) exp(-\int_{t_{j-1}}^{t_j} \lambda(f_j, t_j|H_j)dt) \quad (2)$$

In practical scenarios, to alleviate the complexities associated with jointly and explicitly modeling both the timing and marker information, several studies [5, 7] will factorize the intensity function $\lambda(f, t|H)$ to $\lambda(t|H)p(f|H)$.

4 METHOD

In this section, we present our proposed TPPUM and provide an overview of its architecture. As depicted in Figure 3, given a sequence of previous events, the model first encodes both treatment events and outcome events jointly to obtain their representation ϕ which includes the sequential relations among these events. Subsequently, we leverage the representation ϕ to model the intensity function $\lambda(t|H)$ and the marker's probability $p(f|H)$ by neural network. The intensity function will be further used to predict the timing of the next outcome event. For features of the next outcome event, we construct an outcome predictor to predict them. During the training process, we introduce adversarial learning techniques to ensure that the embedding representation ϕ strikes a balance between being predictive of outcomes and not being predictive of treatments. Finally, we can utilize the estimated intensity function and marker's probability to predict the timing and marker of the next event.

4.1 Balancing Representation Encoding

In order to formulate the process of treatment and outcome events as a unified marked temporal point process, we need to capture the complex dependencies within the historical event sequences based on the sequence encoder. Specifically, we first design two separate mapping functions because of the inherent differences between the features of treatment and outcome events. These functions are responsible for mapping the timing and features of events (f, t) into the embedding $(\mathbf{f}, \mathbf{t})$. Then we feed them into the sequence encoder as depicted in Figure 3 to generate the representation ϕ. To ensure unbiased estimation, it is crucial to obtain the balancing representation ϕ in a manner that is invariant to treatments. We will provide a detailed explanation of how we achieve the balancing encoding in Section 4.4.

4.2 Point Process Learning

As discussed in Section 2.3, we model the marked temporal point process (MTPP) by learning the intensity function $\lambda(t|H)$ and markers' probability $p(f|H)$ based on balancing representation ϕ separately. MTPP stands out for its ability in modeling events within continuous timelines, which is instrumental in accurately capturing the stochastic nature of event timings along with the underlying intensity function. This capability is particularly beneficial for our application, which aims not only to determine the most appropriate treatment options but also to identify the optimal timing for presenting these recommendations to players. The unique ability of MTPP to model time accurately provides flexibility in making treatment decisions about when to offer treatments and what treatments bring in the future, which is particularly critical in addressing the challenges presented by the irregular timing of treatment and outcome events observed in online marketing.

4.2.1 Intensity Learning. For the intensity function $\lambda(t|H)$, previous studies [29, 30] have demonstrated the effectiveness of a multilayer perceptron (MLP) in modeling intensity functions. Building upon these findings, we employ an MLP architecture in this paper to explicitly learn the intensity function. In addition, to avoid the complex calculation of the integral involved in the intensity function, we choose to directly fit the integral of the intensity with neural networks. By obtaining the gradient of the fitted integral with respect to the time, we can effectively estimate the intensity function. The process can be formulated as follows:

$$\begin{aligned} I_t &= \int_{t^-}^{t} \lambda(t|H) \leftarrow \sigma(w_2(\sigma(w_1[\phi; (t - t^-)] + b_1)) + b_2) \\ \lambda(t|H) &= \frac{dI_t}{dt} \end{aligned} \quad (3)$$

where w_1, w_2, b_1, b_2 are trainable parameters of MLP and σ is activation function set as Elu. t^- means the last event's timestamp before the current event. Note that we concatenate ϕ with the time interval $t - t^-$ to feed into MLP because definite integral $\int_{t^-}^{t} \lambda(t|H)$ involves the accumulation from the previous event to the current event in time.

4.2.2 Marker Learning. For the marker's probability, a straightforward solution is to assume the markers' distribution as Gaussian distribution and apply a neural network to fit the parameters of a Gaussian distribution. However, the marker of both treatment and outcome events is not guaranteed to conform to Gaussian distribution. Thus we apply representation learning to derive markers'

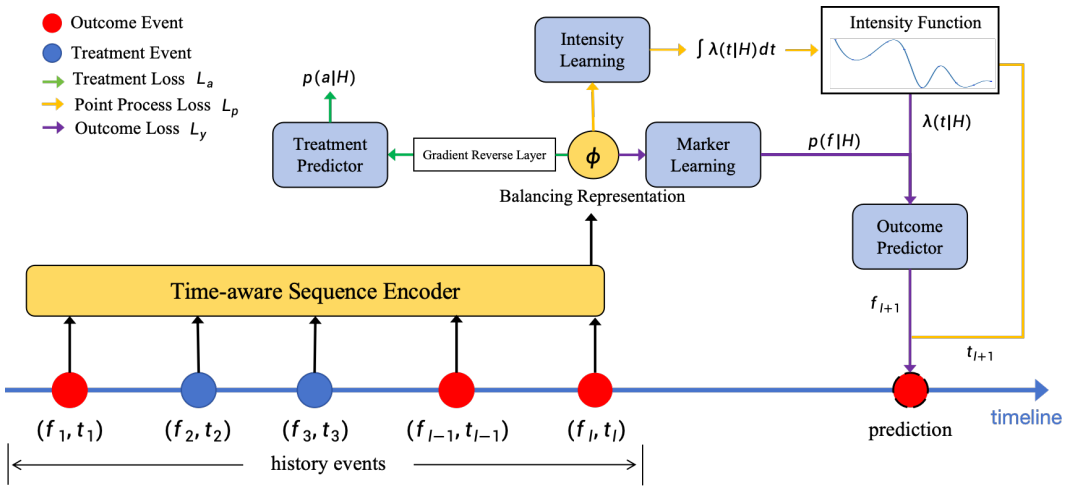

Figure 2: The architecture of TPPUM.

probability from the balancing representation, which can be formulated as:

$$e_d = \sigma(w_4(\sigma(w_3\phi + b_3)) + b_4) \tag{4}$$

where e_d means the representation of markers.

4.3 Marker Prediction

By building an outcome predictor $O(\phi, \lambda, e_d)$, the prediction of markers of the next outcome event can be formulated as follows:

$$\hat{f} = O(\phi, \lambda(t|H), e_d) \tag{5}$$

where $\hat{f} \in R^{d_f}$ means the predicted markers of the next outcome event. Since we focus on the ITE estimation, we only need to use the outcome $\hat{y}$ included in $\hat{f}$ which will be elaborated in section 4.5.

4.4 Training

4.4.1 Point Process Training. Based on Equation (2), the log-likelihood of the marked event (f, t) and point process loss can be formulated as follows:

$$\begin{aligned} logp(f_l, t_l|H) &= log(\lambda(f_l, t_l)exp(-\int_{t_{l-1}}^{t_l} \lambda(f, t|H)dt)) \\ &= log\lambda(f_l, t_l|H) - \int_{t_{l-1}}^{t_l} \lambda(f, t|H)dt \\ &= log\lambda(t_l|H) + logp(f_l|H) - p(f_l|H)\int_{t_{l-1}}^{t_l} \lambda(t|H)dt \\ L_p &= \sum_{i=1}^{N} p(f_l|H)\int_{t_{l-1}}^{t_l} \lambda(t|H)dt - log\lambda(t_l|H) - logp(f_l|H) \end{aligned} \tag{6}$$

As discussed in Section 4.2, we implicitly learn markers' probability $p(f|H)$ by integrating it into the training of outcome predictor which will be elaborated in Section 4.3.2.

4.4.2 Adversarial Training. As discussed in Section 1, the history of events contains the time-varying confounders that bias the treatment assignment in the observational data. Merely minimizing the loss function during model training could result in biased uplift predictions. To tackle this issue, we integrate the domain adversarial technique into the training process with the aim of acquiring a balancing representation denoted ϕ. The objective is to eliminate the future treatment information from ϕ, ensuring that the probability of receiving any specific treatment remains the same for any two users with different historical events. Formally, it can be expressed as $p(a|H_0) = p(a|H_1), \forall a \in treatmentoptions$. Specifically, the adversarial training involves the min-max game:

$$min_\phi max_{\hat{p}} \mathbb{E}_H log\hat{p}(a|\phi(H)) \tag{7}$$

where ϕ represents the representation of historical sequence H and $\hat{p}(a|\phi(H)$ is the prediction of treatment given representation ϕ. According to [4, 30], the solution ϕ ensures $p(\phi(H)|a_1) = p(\phi(H)|a_2)$ for any a_1, a_2 if it reaches Nash balanced.

In practice, the adversarial training approach aims to simultaneously minimize the outcome loss and maximize the treatment loss. To achieve this, we introduce an outcome predictor denoted as $O(\phi, \lambda, e_d)$. Additionally, we construct a treatment classifier denoted as $C(\phi)$. Furthermore, we leverage the Gradient Reversal Layer (GRL) [9] between the balancing representation and the treatment predictor to reverse the sign of the gradient. GRL could facilitate adversarial training during backpropagation. The treatment loss and outcome loss are defined as follows:

$$\begin{aligned} L_a &= \sum_{j=1}^{d_a} \mathbb{I}_{[a=a_j]} log(C(GRL(\phi))) \\ L_y &= ||y - \hat{y}||^2 \\ L_{balance} &= \sum_{i=1}^{N} L_y - \alpha L_a \end{aligned} \tag{8}$$

where α is a hyper-parameter for domain adversarial and N is the number of samples in the dataset. Thereby, the time-varying confounding bias will be removed from balancing representation. Finally, we train the model with the summarization of the loss function including L_p and $L_{balance}$.

Table 1: Statistics of datasets used in this experiment. The statistics of Hawkes-Tumor include all subsets with varying bias coefficients.

Dataset	#Treatment	#Outcome	Avg. Sqe. Len
GAME	1,826,871	432,397	225.9214
Synthetic GAME	1,473,719	1,516,143	158.2913
Hawkes-Tumor	3,691,583	3,581,632	101.0168

4.5 Inference

During the evaluation stage in offline experiments, to estimate the uplift about the next outcome event given current treatment event $\hat{a}$, we follow a two-step process. Firstly, we predict the potential outcomes $\hat{y}(\hat{a})$ and $\hat{y}(0)$ based on the sequence of historical events H, considering the presence or absence of the current treatment event. To estimate the counterfactual outcomes, we conduct this in two scenarios. If the factual treatment option is treated, we remove the last treatment event and construct the counterfactual historical sequence H_{cf}. If the factual treatment option is untreated, we add a simulated treatment event to construct H_{cf}. Its features are consistent with the last factual treatment event and its occurrence time is set to 24 hours after the last event. The counterfactual outcome $\hat{y}(0)$ or $\hat{y}(\hat{a})$ is predicted given H_{cf} Subsequently, we calculate the uplift as the difference between these predicted outcomes, denoted as $\tau(\hat{a}) = \hat{y}(\hat{a}) - \hat{y}(0)$.

On the other hand, in real-world applications, the accurate timing of the next outcome event is not always knowable, that is, we cannot directly predict the outcome as described in Equation 4. To address this limitation, we propose to predict the expected outcome within a specific time window, which can be formulated as follows:

$$E(\hat{y}) = \int_{t}^{t+W} \lambda(t|H)O(\phi, \lambda(t|H))dt \tag{9}$$

where W is a hyper-parameter means the length of the time window. Similarly, we can obtain uplift $\tau(\hat{a})$ by calculating the difference expected outcome $E(\hat{y}(\hat{a}))$ and $E(\hat{y}(0))$.

5 EXPERIMENTS

5.1 Experimental Settings

5.1.1 Baselines. The study of uplift modeling over time applied to temporal event sequences remains unexplored in previous research efforts. To address this research gap, we carefully select a set of methods that demonstrate proficiency in estimating treatment effects based on event sequences over time, including CRN [4], DCRN [2], and CT [19].

- **CRN**: CRN uses adversarial training to construct treatment invariant representation, which aims to address the bias from time-varying confounders.
- **DCRN**: DCRN disentangles the representation of event sequences into three latent factors to allow better time-varying confounder modeling.
- **CT**: CT designs the encoder based on the Transformer and cross-attention network which can model more complex and long-range time-varying confounders.

Since DCRN is only applied to binary treatment scenarios, to evaluate it in multi-treatment scenarios, we make some extendence. Specifically, the origin binary-setting discrepancy measure in the loss function involves the calculation $disc(\mathbf{O}_t^{a=0}, \mathbf{O}_t^{a=1})$, we extend it to the multi-treatment scenario by calculating the distance between two of the multiple $\mathbf{O}_t^a$ and add them together. Furthermore, in order to enable the baselines to leverage temporal information, we have incorporated the time gap from the previous event as an additional input for each time step of the baselines.

5.1.2 Datasets. We conduct the experiments on both the synthetic and real-world data. The statistics of real-world data are presented in Table 1. The generation of synthetic datasets will be described in the Appendix in detail. The datasets include:

- **GAME**: This is real-world industrial data collected from an online game. It includes bundle recommendation logs and users' in-shop purchase logs. Bundle recommendations are treated as the events triggering treatment, while user purchases in the shop are considered as the outcome events.
- **Synthetic GAME**: Motivated by [30], we create a simulation of an online game recommendation scenario. The feature is the same as used in the "GAME" dataset while the distribution is more balanced. Events in the simulation were modeled using a Hawkes process.
- **Hawkes-Tumor**: Followed by [2, 4, 19], we generated Tumor data based on a state-of-the-art biomedical model [10] to simulate the effects of tumor cancer treatments over time. Furthermore, to enhance the consistency of the data with event sequences, the outcome event was simulated as the observation event on tumor growth based on the Hawkes process.

5.1.3 Data Preparation. For GAME datasets, the treatment assignment is selective with high selection bias due to the recommendation strategy, and we use these data as the training set. We also choose another set of users whose treatment assignments are under randomized controlled trials (RCT) and we use them as the test set. For Synthetic GAME datasets, we generated event sequences of 8,000 users for training and another 1,000 users for validation and testing respectively. In this dataset, the feature sets in the GAME for recommendation and purchase events are the same. Consequently, we utilized a single embedding layer to transform these two event types. We choose the prediction of shop revenue to evaluate the prediction performance. In the case of Hawkes-Tumor, we select the time-varying coefficient in $\gamma \in \{0, 1, 3, 5, 7, 10\}$. For each γ, we first simulated 10,000 patients' treatment trajectories and corresponding tumor size data for training, and 1000 patients' data for validation and testing respectively. To enhance this data with time information, we extended the outcome event by introducing observational events linked to tumor size. Subsequently, we sampled timestamps using the Hawkes process to construct an outcome event sequence. The outcome values (tumor size) and treatment were determined based on previous and subsequent knowable events in the sequence. We will elaborate the process in the Appendix.

5.1.4 Metrics. In line with the experimental setup adopted in CRN [4], for the synthetic dataset, we employ two evaluation metrics, namely

Root Mean Square Error (RMSE) and Precision in Estimation of Heterogeneous Effect (pEHE) [1], to assess the performance of models on outcome and uplift predictions. We begin by predicting the outcome value and uplift for each user's outcome event. Subsequently, we calculate the RMSE by comparing the predicted outcome values with the true outcome values. Similarly, we compute pEHE by comparing the predicted uplift values with the true uplift values. For the real-world dataset, the unobservability of the counterfactual outcome prevents us from accessing the true uplift. Consequently, we evaluate the uplift ranking performance using a widely adopted metric in uplift modeling, namely the area under the Qini curve (QINI). Higher Qini indicates the better performance of the model in the uplift task. It should be noticed that although RMSE can be calculated without counterfactual outcomes and measures the prediction of factual outcomes in real-world datasets, it does not provide insights into the effectiveness of uplift modeling, particularly in data with inherent selection bias. This limitation arises because RMSE fails to account for how outcomes vary across different treatment options at the individual level. Consequently, few studies employ RMSE in real-world datasets.

5.1.5 Implementation Details. We implement our model in PyTorch 1.10.1. We use an Adam optimizer and set the number of epochs to 100. During validation, we use RMSE as the evaluation metric for searching the best hyper-parameters. To ensure the robustness and reliability of our evaluations, we conducted each experiment five times and computed the average results.

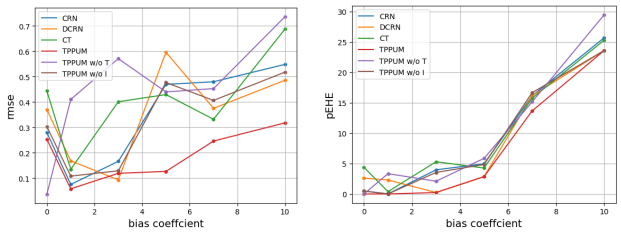

(a) (b)

Figure 3: Results on Hawkes-Tumor dataset with varying degree of bias coefficient γ. A higher γ value indicates a greater presence of bias within the dataset.

5.2 Performance Evaluation

Because the Hawkes Tumor dataset has 6 subsets with different bias coefficients λ, we depict the comparison results on the Hawkes Tumor dataset in Figure 3 for direct visualization and show results on the GAME and synthetic GAME datasets in Table 2. In real-world scenarios, we are often limited to observing only one potential outcome. However, using synthetic data offers a distinct advantage by providing access to counterfactual outcomes. This unique capability empowers us to explicitly evaluate the predictions of counterfactual outcomes, enabling a comprehensive assessment of models. Note that the RMSE in Figure 3 is normalized by the maximum tumor volume 1150. From the results in Figure 3, we can have the following observations:

Table 2: The results of the comparison methods on Synthetic GAME dataset and real-world GAME dataset. The best performance on each dataset is highlighted with bold font.

Dataset	Synthetic GAME		GAME
Metric	Average RMSE	Average pEHE	Qini
CRN	27.3875	45.4682	0.0190
DCRN	32.3839	54.6399	0.0157
CT	29.1003	44.5813	0.0097
TPPUM w/o T	25.1069	40.5218	-0.0111
TPPUM w/o I	26.8344	43.4867	0.0031
TPPUM	**23.2204**	**36.8538**	**0.0205**
Improv	8.8470%	17.3335%	7.8947%

- CT performs poorly among all baselines in most cases. It may be attributed to the complicated architecture of its attention-based encoder. Especially in Synthetic GAME, The time-dependent confounding introduced by complex, feature-laden treatments and treatment sequences leads to a higher risk of overfitting for CT.
- Our TPPUM consistently outperforms all baselines on two Synthetic datasets in most cases. Especially when bias coefficient $\gamma = 10$, TPPUM improves by 34.57% on RMSE. While CRN and DCRN also employ RNN for encoding event sequences within the counterfactual framework, TPPUM surpasses them by adopting a distinctive approach that treats users' event sequences as uniform marked point processes. This unique methodology effectively alleviates the challenges associated with the distribution of continuous-time events in complex scenarios of online marketing. Furthermore, our model excels in enhancing predictions of the next events on the timeline, resulting from its incorporation of intensity function and markers' distribution representations. This augmentation provides a distinct advantage compared to relying solely on the neural network-based predictor.

For the real-world GAME dataset, the Qini score measures the ranking performance according to predicted uplift and is applied in areas where ground truth uplift is unknown. As shown in Table 2, our proposed TPPUM surpasses the best baselines by 8.8470%, 17.3335% and 7.8947% on RMSE, pEHE and Qini respectively. Similar to the performance in Synthetic data, CT still suffers from its complicated encoder and achieves the worst performance. Our TPPUM consistently outperforms other baselines in the GAME dataset. This achievement stems from the model's ability to efficiently capture the dynamics of users' events along the timeline through point process modeling. The results of previous experiments validate the significant effectiveness of TPPUM in the uplift task.

5.3 Ablation Study

Moreover, we conduct ablation studies of our TPPUM to analyze the importance of each part. We consider the following variants of TPPUM.

- **TPPUM w/o T**: A model variant that removes adversarial balancing representation learning.

- **TPPUM w/o I**: A model variant that removes intensity learning from outcome prediction.

The results are shown in Figure 3 and Table 2. Specifically, when removing adversarial training to conduct balancing encoding of event sequences, the model performance has a decline. It is mainly due to the bias from time-varying confounders that confuse the model on the treatment effect. A surprising phenomenon is that even after removing the balancing encoding, TPPUM w/o T still outperforms baselines in the synthetic GAME dataset. We speculate that the reason is a relatively lower treatment bias in the Synthetic GAME dataset compared to other datasets and thus the variant could retain a great performance via point process learning. When the model removes the intensity from point process learning and only preserves the marker for outcome prediction, it will also bring performance degradation. This validates the effectiveness of intensity learning, i.e., the estimated intensity can provide a mathematical characterization of the distribution of future event occurrences, which is crucial for counterfactual outcome prediction.

6 ONLINE DEPLOYMENT

We applied our proposed TPPUM in one of the most popular games[1] released by *NetEase Games*[2] for providing online marketing service by recommending discounted bundles to users. Figure 4 presents a graphical process of the application. There are two types of user purchase events: one involves users purchasing the recommended discounted bundle at a reduced price, while the other involves users making purchases at the original price in the in-game shop. The latter can be considered as user-initiated purchases resulting from spontaneous demand. User interaction with the application is divided into four parts. Firstly, during the gameplay, users may trigger bundle treatment due to various predefined conditions with an approximate frequency of 30 times per day (Step 1). The strategy will determine whether to make an intervention (Step 2) and then decide the contents of the discounted bundle (Step 3). The bundle consists of multiple item IDs and their corresponding item quantities, and the discount is determined by manual rules. Note that bundle treatments are limited to an average of 3~4 opportunities per day, not every user-triggered event will result in a recommendation. This necessitates the need for decision-making regarding the timing of interventions. Then user will receive a pop-up window and have 30 minutes to decide whether to make a purchase. Undoubtedly, the recommendation of discounted bundles (i.e., treatment) will influence user spending in the in-game shop (i.e., outcomes) through substitution effects and demand stimulation effects. Therefore, for this online marketing problem, we need to dynamically select the optimal treatment and timing based on real-time user context to maximize the total Gross Merchandise Volume (GMV) from bundle sales and shop transactions. This relies on accurately estimating the counterfactual uplift of treatments.

During a two-week online A/B testing, we conducted a comparative analysis of Transformer [27], CRN [4], and TPPUM. Transformer is the existing baseline without uplift prediction. It was

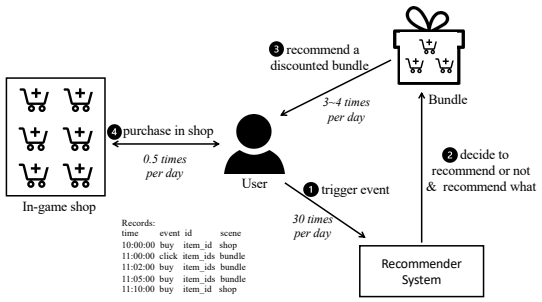

Figure 4: A graphic description of the discounted bundle recommendation service. The application includes two scenarios: discounted bundle and in-game shop.

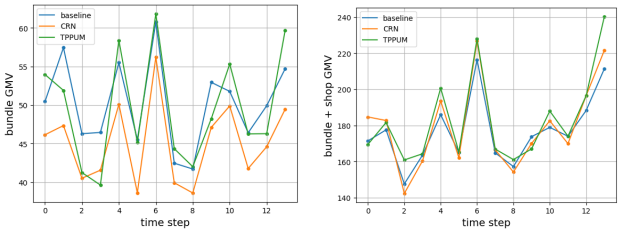

Figure 5: Results of the two-week online A/B testing. The left and right parts illustrate the revenue from discounted bundles and the application-level revenue, respectively.

previously employed in live deployment, with a primary focus on maximizing revenue in gift bundle scenarios. On the other hand, CRN represents a widely-used causal inference algorithm for sequential treatment but is limited to discrete time series and 1-step outcome prediction. To enable compatibility with CRN, we defined a time step as three hours and consolidated multiple treatments occurring within the same time step. In the uplift inference phase of CRN, the objective was formulated to maximize the revenue from the current time step's treatment, combined with the outcome revenue (i.e., the in-game shop). The uplift inference process of TPPUM has been described in Section 4.5. We set the time window W to be 24 hours. The TPPUM network's single inference time is 100-150 milliseconds with a GPU device and 300-400 milliseconds with a CPU device. As depicted in Figure 5, the results from a 14-day A/B test indicate that, compared to the baseline scenario of only optimizing the bundle, TPPUM suffered a certain loss in GMV within the bundle scenario. This loss, however, was compensated by a growth in the overall GMV of bundle plus shop (3.6%). On the other hand, CRN adopted a more aggressive strategy. However, a higher loss in bundle GMV (-8.9%) did not lead to a higher shop GMV, resulting in a decrease in the overall GMV of bundle plus shop by 1.8%. On Sundays (the 6th and the 13th day), TPPUM achieved significant growth in both bundle and shop compared to other baselines by providing bundles with only smaller discounts. This demonstrates that TPPUM accurately estimated the uplift of discount bundle sequence on users' purchase behavior in in-game

[1]The game is a real-world production game. Its name is kept anonymous during the review stage
[2]http://leihuo.163.com/en/index.html

shop, thus enabling the selection of the best treatment and recommendation timing, ultimately leading to an increase in overall user purchases in both scenarios.

7 CONCLUSION

In this paper, to address the task of uplift estimation in complex marketing scenarios, where users receive multiple interventions over time, we propose a temporal point process-based uplift modeling network, named TPPUM. By modeling the historical events sequence as a marked temporal point process, we estimate the future intensity and the markers' based on balancing representation. Here, the model could evaluate the treatment effect on individual users by event prediction. We deployed the model into a real-world online marketing application with a significant improvement. The combination of causal inference and more sophisticated time-series point process methods will be one of the future research directions.

ACKNOWLEDGMENTS

This work was supported by the National Key Research and Development Program of China 2023YFC2705700, National Natural Science Foundation of China under Grants 62225113, 62271357, Natural Science Foundation of Hubei Province under Grants 2023BAB072, the Innovative Research Group Project of Hubei Province under Grants 2024AFA017, and the Fundamental Research Funds for the Central Universities under Grants 2042023kf0134.

REFERENCES

[1] Susan Athey, Guido W Imbens, and Stefan Wager. 2018. Approximate residual balancing: debiased inference of average treatment effects in high dimensions. *Journal of the Royal Statistical Society Series B: Statistical Methodology* 80, 4 (2018), 597–623.

[2] Jeroen Berrevoets, Alicia Curth, Ioana Bica, Eoin McKinney, and Mihaela van der Schaar. 2021. Disentangled counterfactual recurrent networks for treatment effect inference over time. *arXiv preprint arXiv:2112.03811* (2021).

[3] Artem Betlei, Eustache Diemert, and Massih-Reza Amini. 2021. Uplift modeling with generalization guarantees. In *Proceedings of the 27th ACM SIGKDD Conference on Knowledge Discovery & Data Mining*. 55–65.

[4] Ioana Bica, Ahmed M Alaa, James Jordon, and Mihaela van der Schaar. 2019. Estimating counterfactual treatment outcomes over time through adversarially balanced representations. In *International Conference on Learning Representations*.

[5] Ricky TQ Chen, Brandon Amos, and Maximilian Nickel. 2020. Neural spatio-temporal point processes. *arXiv preprint arXiv:2011.04583* (2020).

[6] Floris Devriendt, Jente Van Belle, Tias Guns, and Wouter Verbeke. 2020. Learning to rank for uplift modeling. *IEEE Transactions on Knowledge and Data Engineering* 34, 10 (2020), 4888–4904.

[7] Nan Du, Hanjun Dai, Rakshit Trivedi, Utkarsh Upadhyay, Manuel Gomez-Rodriguez, and Le Song. 2016. Recurrent marked temporal point processes: Embedding event history to vector. In *Proceedings of the 22nd ACM SIGKDD international conference on knowledge discovery and data mining*. 1555–1564.

[8] Garrett Fitzmaurice, Marie Davidian, Geert Verbeke, and Geert Molenberghs. 2008. Estimation of the causal effects of time-varying exposures. In *Longitudinal Data Analysis*. Chapman and Hall/CRC, 567–614.

[9] Yaroslav Ganin, Evgeniya Ustinova, Hana Ajakan, Pascal Germain, Hugo Larochelle, François Laviolette, Mario Marchand, and Victor Lempitsky. 2016. Domain-adversarial training of neural networks. *The journal of machine learning research* 17, 1 (2016), 2096–2030.

[10] Changran Geng, Harald Paganetti, and Clemens Grassberger. 2017. Prediction of treatment response for combined chemo-and radiation therapy for non-small cell lung cancer patients using a bio-mathematical model. *Scientific reports* 7, 1 (2017), 13542.

[11] Maciej Jaskowski and Szymon Jaroszewicz. 2012. Uplift modeling for clinical trial data. In *ICML Workshop on Clinical Data Analysis*, Vol. 46. 79–95.

[12] Wang-Cheng Kang and Julian McAuley. 2018. Self-attentive sequential recommendation. In *2018 IEEE international conference on data mining (ICDM)*. IEEE, 197–206.

[13] Sören R Künzel, Jasjeet S Sekhon, Peter J Bickel, and Bin Yu. 2019. Metalearners for estimating heterogeneous treatment effects using machine learning. *Proceedings of the national academy of sciences* 116, 10 (2019), 4156–4165.

[14] Bryan Lim. 2018. Forecasting treatment responses over time using recurrent marginal structural networks. *Advances in neural information processing systems* 31 (2018).

[15] Ying-Chun Lin, Chi-Hsuan Huang, Chu-Cheng Hsieh, Yu-Chen Shu, and Kun-Ta Chuang. 2017. Monetary discount strategies for real-time promotion campaign. In *Proceedings of the 26th International Conference on World Wide Web*. 1123–1132.

[16] Dugang Liu, Xing Tang, Han Gao, Fuyuan Lyu, and Xiuqiang He. 2023. Explicit Feature Interaction-aware Uplift Network for Online Marketing. *arXiv preprint arXiv:2306.00315* (2023).

[17] Christos Louizos, Uri Shalit, Joris M Mooij, David Sontag, Richard Zemel, and Max Welling. 2017. Causal effect inference with deep latent-variable models. *Advances in neural information processing systems* 30 (2017).

[18] Hongyuan Mei and Jason M Eisner. 2017. The neural hawkes process: A neurally self-modulating multivariate point process. *Advances in neural information processing systems* 30 (2017).

[19] Valentyn Melnychuk, Dennis Frauen, and Stefan Feuerriegel. 2022. Causal transformer for estimating counterfactual outcomes. In *International Conference on Machine Learning*. PMLR, 15293–15329.

[20] Xinkun Nie and Stefan Wager. 2021. Quasi-oracle estimation of heterogeneous treatment effects. *Biometrika* 108, 2 (2021), 299–319.

[21] Donald B Rubin. 2005. Causal inference using potential outcomes: Design, modeling, decisions. *J. Amer. Statist. Assoc.* 100, 469 (2005), 322–331.

[22] Piotr Rzepakowski and Szymon Jaroszewicz. 2010. Decision trees for uplift modeling. In *2010 IEEE International Conference on Data Mining*. IEEE, 441–450.

[23] Uri Shalit, Fredrik D Johansson, and David Sontag. 2017. Estimating individual treatment effect: generalization bounds and algorithms. In *International conference on machine learning*. PMLR, 3076–3085.

[24] Karishma Sharma, Yizhou Zhang, Emilio Ferrara, and Yan Liu. 2021. Identifying coordinated accounts on social media through hidden influence and group behaviours. In *Proceedings of the 27th ACM SIGKDD Conference on Knowledge Discovery & Data Mining*. 1441–1451.

[25] Claudia Shi, David Blei, and Victor Veitch. 2019. Adapting neural networks for the estimation of treatment effects. *Advances in neural information processing systems* 32 (2019).

[26] Xiaogang Su, Joseph Kang, Juanjuan Fan, Richard A Levine, and Xin Yan. 2012. Facilitating score and causal inference trees for large observational studies. *Journal of Machine Learning Research* 13 (2012), 2955.

[27] Ashish Vaswani, Noam Shazeer, Niki Parmar, Jakob Uszkoreit, Llion Jones, Aidan N Gomez, Łukasz Kaiser, and Illia Polosukhin. 2017. Attention is all you need. In *Advances in neural information processing systems*. 6000–6010.

[28] Jinsung Yoon, James Jordon, and Mihaela Van Der Schaar. 2018. GANITE: Estimation of individualized treatment effects using generative adversarial nets. In *International conference on learning representations*.

[29] Kanghoon Yoon, Youngjun Im, Jingyu Choi, Taehwan Jeong, and Jinkyoo Park. 2023. Learning Multivariate Hawkes Process via Graph Recurrent Neural Network. In *Proceedings of the 29th ACM SIGKDD Conference on Knowledge Discovery and Data Mining*. 5451–5462.

[30] Yizhou Zhang, Defu Cao, and Yan Liu. 2022. Counterfactual neural temporal point process for estimating causal influence of misinformation on social media. *Advances in Neural Information Processing Systems* 35 (2022), 10643–10655.

[31] Kui Zhao, Junhao Hua, Ling Yan, Qi Zhang, Huan Xu, and Cheng Yang. 2019. A unified framework for marketing budget allocation. In *Proceedings of the 25th ACM SIGKDD International Conference on Knowledge Discovery & Data Mining*. 1820–1830.

[32] Kailiang Zhong, Fengtong Xiao, Yan Ren, Yaorong Liang, Wenqing Yao, Xiaofeng Yang, and Ling Cen. 2022. DESCN: Deep Entire Space Cross Networks for Individual Treatment Effect Estimation. In *Proceedings of the 28th ACM SIGKDD Conference on Knowledge Discovery and Data Mining*. 4612–4620.

[33] Tengfei Zhou, Hui Qian, Zebang Shen, Chao Zhang, Chengwei Wang, Shichen Liu, and Wenwu Ou. 2018. JUMP: a joint predictor for user click and dwell time. In *Proceedings of the 27th International Joint Conference on Artificial Intelligence. AAAI Press*. 3704–3710.

Algorithm 1: Generation process of synthetic GAME

Randomly generate embedding of users and items and the parameters of $f_{gift}(), f_{shop}(), f_{value}()$
Set hyper-parameter a and b to control the ratio between two events and counterfactual treatment options respectively
for *each user* u **do**
  $H = \varnothing$
  while t_{cur} < *ending time* T **do**
    Draw an in-shop purchase event timestamp t_s and features f_s based on $\lambda_s(f, t|H)$ between t_{curr} and T
    Draw a gift bundle recommendation event timestamp t_g and features f_g based on $\lambda_g(f, t|H)$ between t_{curr} and T
    if $t_g < t_s + a$ **then**
      flag = 'Treatment'
      Draw a gift bought label *label* based on $p_g(f_g|H)$
      $H = H \cup (f_g, t_g, label)$
      $t_{curr} = t_g$
    else
      flag = 'Outcome'
      if *last event in* H *is gift recommendation event* **then**
        $H_{cf} = H - lastevent$
      else
        $f_{cf} = f_s$ except discount in f_{cf} is 0.5
        $t_{cf} = max(lastevent'stimestamp, t_s - b)$
        $H_{cf} = H \cup (f_{cf}, t_{cf}, 1)$
        $p_{cf}(y|t_{cf}, H_{cf}) = \lambda_s(y, t_{cf}|H_{cf}) / \int \lambda_s(y, t_{cf}|H_{cf})dy$
        Sample counterfactual outcome y_{cf} based on distribution $p_{cf}(y|t_{cf}, H_{cf})$
      Actual outcome y set as price in f_s
      $label = 1$ $H = H \cup (f_s, t_s, label, y, y_{cf})$ $t_{curr} = t_s$

Algorithm 2: Generation process of Hawkes-Tumor

Simulate Initial Tumor data with counterfactual outcomes
for *each user* u **do**
  $H = \varnothing$
  while t_{cur} < *ending time* T **do**
    Draw an observation event timestamp t_o based on $\lambda_o(t|H)$ between t_{curr} and T
    denote last time step before t_o as p-th step
    $y_{curr} = y_p + (t_{curr} - t_p)(y_{p+1} - y_p)$
    $y^{cf}_{curr} = y_p + (t_{curr} - t_p)(y^{cf}_{p+1} - y^{cf}_p)$
    $H = H \cup (a_p, t_p) \cup (y_{curr}, y^{cf}_{curr}, t_{curr})$

A SYNTHETIC DATASET GENERATION

In the experiment, we use two synthetic datasets including the synthetic GAME dataset and the Hawkes-Tumor dataset. In this section, we introduce how to generate these two datasets based on the Hawkes process.

A.1 Synthetic GAME

In the generation of Synthetic GAME, motivated by [30] that uses hidden vectors to represent users and news and simulate the sequence of users by modeling Hawkes process. On the basis of this idea, we first randomly initialize the embeddings of users u and items i and the parameters of various functions and then define the intensity function of the gift bundle recommendation event and in-shop purchase event as:

$$\begin{aligned}\lambda_g(f_g, t_g|H) &= uf_{gift}(f_g) + \sum_{(f_l,t_l)\in H} e^{t_l - t} f_{value}(f_{gift}(f_l)) \\ \lambda_s(f_s, t_s|H) &= uf_{shop}(f_s) + \sum_{(f_l,t_l)\in H} e^{t_l - t} f_{value}(f_{shop}(f_l * label))\end{aligned} \tag{10}$$

where f_g, f_s are features of gift bundle recommendation and in-shop purchase events including items' embedding, number of items and discount. H denotes the historical events including both gift bundle recommendations and in-shop purchases. *label* indicates if items are purchased. $f_{gift}()$ and $f_{shop}()$ transform the event's features to the representation of values of items. $f_{value}()$ ensures items' value in history events are measurable in Hawkes process. Additionally, unlike in-shop purchase events, the results of gift bundle recommendations are classified as bought and not bought. We extra define the probability of recommended gifts bought by users as:

$$p_g(f_g|H) = sigmoid(uf_{value}(f_g) + \frac{1}{L} \sum_{(f_l,t_l)\in H} (f_{value}(f_l)) + noise \tag{11}$$

The process is described in Algorithm 1.

A.2 Hawkes-Tumor

In the generation of Hawkes-Tumor, we first simulate patients' data following [4]. For l-th time step t_l, a patient has the corresponding tumor size y_l, treatments a_l and counterfactual tumor y^{cf}_l size with other treatment options. Then we define the outcome event as the observation of tumor size. The intensity function of the outcome event can be defined as:

$$\lambda_o(t|H) = I_{base} + \sum_{t_l\in H} \alpha(e^{\beta(t_l - t)})) \tag{12}$$

where I_{base} is a randomly generate base intensity and α, β are hyper-parameters. The process is described in Algorithm 2.